Landau-Zener Bloch Oscillations with Perturbed Flat Bands

Ramaz Khomeriki[1,2] and Sergej Flach[2,3]
[1]Physics Department, Tbilisi State University, Chavchavadze 3, 0128 Tbilisi, Georgia
[2]Center for Theoretical Physics of Complex Systems, Institute for Basic Science, Daejeon 34051, South Korea
[3]New Zealand Institute for Advanced Study, Centre for Theoretical Chemistry & Physics, Massey University, Auckland 0745, New Zealand

(Received 28 February 2016; published 15 June 2016)

Sinusoidal Bloch oscillations appear in band structures exposed to external fields. Landau-Zener (LZ) tunneling between different bands is usually a counteracting effect limiting Bloch oscillations. Here we consider a flat band network with two dispersive and one flat band, e.g., for ultracold atoms and optical waveguide networks. Using external synthetic gauge and gravitational fields we obtain a perturbed yet gapless band structure with almost flat parts. The resulting Bloch oscillations consist of two parts—a fast scan through the nonflat part of the dispersion structure, and an almost complete halt for substantial time when the atomic or photonic wave packet is trapped in the original flat band part of the unperturbed spectrum, made possible due to LZ tunneling.

DOI: 10.1103/PhysRevLett.116.245301

Lattice waves probe the symmetries and topologies imprinted by an underlying periodic potential. Quite often it is possible to restrict the dynamics to a few bands, for instance for electrons in crystals or in artificial quantum dot arrays [1], ultracold atoms in optical lattices [2], microwaves in dielectric resonator networks [3], and light propagation in waveguide networks [4]. Additional interactions between the constituent waves lead to interesting new phenomena (see references in recent reviews on topological flat bands [5,6]).

Flat band (FB) networks are specific tight-binding translationally invariant lattices with local symmetries which ensure the existence of one (or a few) completely dispersionless bands in the spectrum. FBs have been studied in a number of lattice models in three-dimensional, two-dimensional, and even one-dimensional (1D) settings [7–9], and recently realized experimentally with photonic waveguide networks [10–12], exciton-polariton condensates [13,14], and ultracold atomic condensates [15,16].

FB networks rely on the existence of compact localized eigenstates (CLS) due to destructive interference, enabled by the local symmetries of the network. FB networks are constructed using graph theory [7,17–20] and CLS [7,21,22] and can be perturbed e.g., by disorder to arrive at unexpected new scaling laws [22,23], and correlated potentials to arrive at diverging densitites of states, gaps, and designable mobility edges [24,25]. A perhaps most prominent example is the fractional quantum Hall effect, which occurs as a result of the flat band degeneracy of Landau levels of electrons in a magnetic field and electron-electron interactions [26]. Compact localized eigenstates have been recently successfully obtained in experiments with photonic waveguide networks [11,12] and exciton-polariton condensate networks [14]. Therefore CLS are addressable states in a flat band system.

A very intriguing question which might be important for applications is whether and how compact localized states will perform Bloch oscillations in the presence of external fields. To address this question we choose the diamond chain FB network in Fig. 1 with a flat band which intersects dispersive bands [22]. This model has an easily realizable geometry, as can be observed from published experimental realizations of one- and two-dimensional Lieb lattices [10–14], which are topologically very close to the diamond chain considered here.

We perturb the FB of the diamond chain network and hybridize it with dispersive modes under the action of dc electric and magnetic fields in a two-dimensional setting (the case of magnetic fields only was considered in [27]). Our results are applicable for ultracold atoms in optical lattices where the electric field is substituted by a tilt of the lattice in the gravitational field [28] or accelerating the whole lattice [29], while the magnetic field is generated by artificial gauge fields [30]. Notably the same type of perturbations can be arranged in optical waveguide arrays

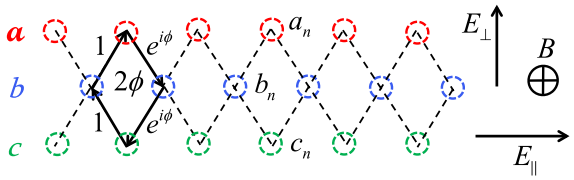

FIG. 1. Schematics for the three leg diamond lattice with a (red), b (blue), and c (green) legs. Dashed lines indicate sites connected with hopping (tunneling) of the quantum particle (wave). Solid arrows indicate the phase of complex hopping constants in a single plaquette, with the specific gauge used for the perpendicular (to the lattice plane) dc magnetic field B. $E_\parallel$ and $E_\perp$ define the longitudinal and transversal components of the dc electric field, respectively.

where the electric field is modeled by a curved geometry of the waveguides [31], while a special metallic fabrication of the waveguides and the surrounding medium [32] mimics a magnetic flux.

The applied dc field only partly removes the flatness of the FB leading to a gapped band structure. A properly added magnetic flux closes these gaps and enforces Landau-Zener tunneling [33] which scans the whole band structure in Bloch oscillation manner [34], and comes to an almost complete halt once the wave is exploring the reminders of the unperturbed flat band.

The tight-binding Hamiltonian of the diamond chain (Fig. 1) reads as follows:

$$\begin{aligned}
\hat{\mathcal{H}} &= \hat{\mathcal{H}}_h + \hat{\mathcal{H}}_\perp + \hat{\mathcal{H}}_\parallel, \\
\hat{\mathcal{H}}_h &= -\sum (\hat{b}_n^+ \hat{a}_n + \hat{c}_n^+ \hat{b}_n) e^{i\phi} - \hat{b}_{n-1}^+ \hat{c}_n - \hat{a}_n^+ \hat{b}_{n-1} + \text{c.c.}, \\
\hat{\mathcal{H}}_\perp &= \sum E_\perp (\hat{a}_n^+ \hat{a}_n - c_n^+ \hat{c}_n), \\
\hat{\mathcal{H}}_\parallel &= \sum E_\parallel n (\hat{a}_n^+ \hat{a}_n + \hat{b}_n^+ \hat{b}_n + \hat{c}_n^+ \hat{c}_n) + \frac{E_\parallel}{2} \hat{b}_n^+ \hat{b}_n, \qquad (1)
\end{aligned}$$

where $\hat{a}_j^+$, $\hat{b}_j^+$, $\hat{c}_j^+$ and $\hat{a}_j$, $\hat{b}_j$, $\hat{c}_j$ are standard creation and annihilation operators of an atom at the jth lattice site of the legs a, b, c, but could also simply be complex amplitudes of a photonic light field in a waveguide structure. $E_\parallel$ and $E_\perp$ are longitudinal and transversal in-plane components of a dc electric (gravitational) field which detunes the on-site energies of the network. The phase ϕ complexifies the tunneling amplitudes as a particular gauge choice for the dc magnetic (artificial gauge) field B which is oriented perpendicular to the diamond chain embedding plane. It follows that the magnetic flux penetrating each diamond plaquette has the value 2ϕ.

The discrete Schrödinger equation which follows from (1) is given by

$$\begin{aligned}
i\dot{a}_n &= (E_\parallel n + E_\perp) a_n - e^{-i\phi} b_n - b_{n-1}, \\
i\dot{b}_n &= E_\parallel \left(n + \frac{1}{2}\right) b_n - e^{i\phi} a_n - e^{-i\phi} c_n - c_{n+1} - a_{n+1}, \\
i\dot{c}_n &= (E_\parallel n - E_\perp) c_n - e^{i\phi} b_n - b_{n-1}. \qquad (2)
\end{aligned}$$

In the absence of a longitudinal field $E_\parallel = 0$ we seek for plane wave solutions $a_n = a(t)e^{ikn}$, $b_n = b(t)e^{ikn}$, $c_n = c(t)e^{ikn}$:

$$\begin{aligned}
i\dot{a} &= E_\perp a - (e^{-i\phi} + e^{-ik}) b, \\
i\dot{b} &= -(e^{i\phi} + e^{ik}) a - (e^{-i\phi} + e^{ik}) c, \\
i\dot{c} &= -E_\perp c - (e^{i\phi} + e^{-ik}) b, \qquad (3)
\end{aligned}$$

and arrive at the following cubic equation for the eigenvalue λ using $a(t), b(t), c(t) \sim e^{i\lambda t}$:

$$\begin{aligned}
&-\lambda^3 + C\lambda - D = 0, \\
&C = E_\perp^2 + 4(1 + \cos\phi \cos k), \\
&D = 4E_\perp \sin\phi \sin k. \qquad (4)
\end{aligned}$$

For special cases it follows that one central (at $\lambda = 0$) or all three bands are flat [27] and shown in Figs. 3(a) and 3(c):

$$\begin{aligned}
&\phi = 0 \;:\quad \lambda_1 = 0, \qquad \lambda_\pm = \pm\sqrt{E_\perp^2 + 4(1 + \cos k)}, \\
&E_\perp = 0, \quad \phi = \pi/2 \;:\quad \lambda_1 = 0, \quad \lambda_\pm = \pm 2, \\
&E_\perp = 0 \;:\quad \lambda_1 = 0, \qquad \lambda_\pm = \pm 2\sqrt{1 + \cos\phi \cos k}. \qquad (5)
\end{aligned}$$

Apart from those cases, all bands are nonflat, with a typical dispersion shown in Fig. 3(d). The central flatband becomes dispersive, and we observe two gaps (avoided crossings) symmetrically located around $k = \pi$ and $\lambda = 0$. In the absence of both fields [Fig. 3(a)], or in the presence of only one of the two fields [Figs. 3(b) and 3(c)], the band structure appears to be invariant under either the particle-hole symmetry operation $\lambda \to -\lambda$ or the time (or space) reversal operation $k \to -k$, even in the presence of a magnetic field. This is because the eigenvectors, and the equations (3) are invariant under the following symmetries: $\phi = 0$: $t \to -t$, $k \to -k$, complex conjugation; $\phi \neq 0$: $t \to -t$, $k \to -k$, $a(b) \to b(a)$, complex conjugation. Since $E_\perp$ detunes the a and b sites, this leads to a lower spectral symmetry of the general case in Fig. 3(d) where the spectrum is invariant under the combined action of both $\lambda \to -\lambda$ and $k \to -k$ operations.

The Bloch eigenstates of a flat band can be superposed in order to obtain compact localized eigenstates [22]. Different flatband networks are characterized by different local symmetries and topologies of CLS. In one-dimensional settings the CLS can be classified by the integer number U of unit cells they occupy [22]. For $U = 1$ CLS form an orthogonal linearly independent set, while for $U > 1$ their set is linearly independent but nonorthogonal. For a given network the value of U can change upon lowering local symmetries, e.g., due to external fields. For $E_\perp = \phi = 0$ the diamond chain belongs to the $U = 1$ class, and its irreducible compact localized state is shown in Fig. 2(a). Only two sites within one unit cell are occupied. Destructive interference prevents a leaking of the wave functions into the exterior. For all other flat band cases considered in (5) the CLS class increases to $U = 2$. For $\phi = 0$ the CLS at $\lambda = 0$ is shown in Fig. 2(b). Note that this CLS will tend to a single site $U = 1$ CLS in the limit of infinite $E_\perp$. For $E_\perp = 0$ and nonzero flux ϕ the CLS vector becomes complex as shown in Fig. 2(c) at $\lambda = 0$. For the special case $\phi = \pi/2$ all three bands turn flat [27] and the new flat band energies $\lambda = \pm 2$ correspond to the CLS vectors shown in Fig. 2(d).

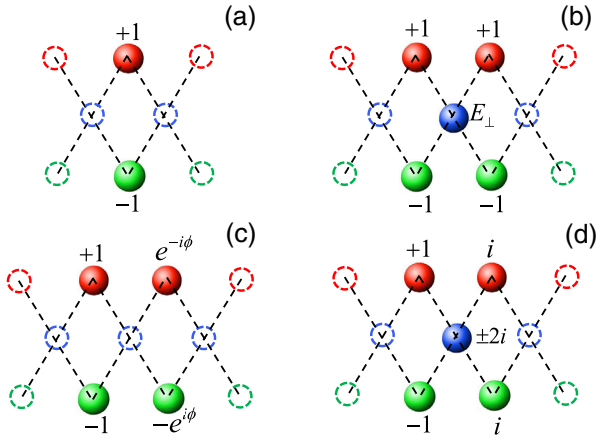

FIG. 2. CLS structure. Filled circles designate occupied sites with amplitudes denoted right to them, which have to be divided by a factor n to ensure normalization of the eigenvector. Empty circles correspond to zero amplitudes. Lines indicate the hopping connections. (a) $E_\perp = \phi = 0$, $\lambda = 0$, $n = \sqrt{2}$; (b) $\phi = 0$, $\lambda = 0$, $n = \sqrt{4 + E_\perp^2}$; (c) $E_\perp = 0$, $\lambda = 0$, $n = 2$; (d) $E_\perp = 0$, $\phi = \pi/2$, $\lambda = \pm 2$, $n = \sqrt{8}$. The color definitions are as in Fig. 1.

By fine-tuning the parameters $E_\perp$ and ϕ we can close the gaps in the band structure completely. Indeed, the cubic equation (4) has two degenerate roots when the Cardano equality $4C^3 = 27D^2$ is satisfied, which translates into

$$E_\perp^2 + 4(1 + \cos\phi\cos k) = (6/2^{1/3})(E_\perp \sin\phi \sin k)^{2/3}. \quad (6)$$

Let us take ϕ as the free variable. It is straightforward to show that there is a solution to (6) which is given by

$$E_\perp = \sqrt{2}\sin\phi, \qquad k = \pi \pm \phi. \quad (7)$$

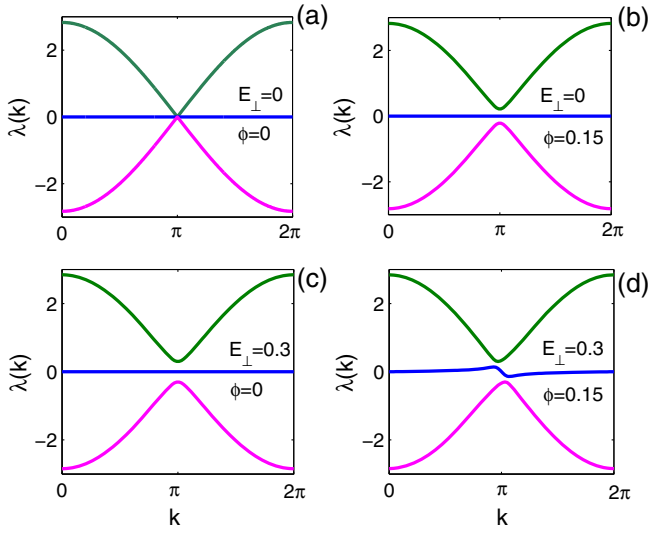

FIG. 3. Band energies versus wave number. Graph (a) displays the case when transversal fields are absent, in (b) and (c) one of the fields is present, while in graph (d) both dc electric and magnetic fields are nonzero. The parameter values are indicated in the graphs.

The band structure with vanishing gaps for the particular value of $\phi = 0.2$ is shown in Fig. 5(a). The perturbed flat band part still displays a significant portion which is almost dispersionless.

Next we consider the case $E_\parallel \neq 0$. We note that the CLS for $E_\perp = \phi = 0$ in Fig. 2(a) is still an exact solution of the wave equations in the presence of nonzero $E_\parallel$, and any linear combination of multiple CLS as well [35]. We will therefore first consider a Gaussian wave packet of such linear CLS combinations $a_n = -c_n = e^{-n^2/2\sigma^2}$ as an initial state with variance $\sigma = 70$, and trace its evolution for $E_\parallel = 0.05$. Figure 3 shows the band structure for four different parameter cases, and Fig. 4 the evolution of the norm density per unit cell $\rho_n = |a_n|^2 + |b_n|^2 + |c_n|^2$. In all considered cases we observe Bloch oscillations. However, the details of these oscillations are strongly depending on the different cases considered.

The above mentioned case $E_\perp = \phi = 0$ with a flat band at $\lambda = 0$ [Fig. 3(a)] keeps the compactness of the initial state; therefore, no oscillations occur [Fig. 4(a)]. For $E_\perp = 0$ and $\phi \neq 0$ and similarly for $E_\perp \neq 0$ and $\phi = 0$ the initial state starts to evolve in a symmetric way [Figs. 4(b) and 4(c)] reflecting the band structure symmetry in Figs. 3(b) and 3(c), and the fact that the initial state ceases to be a linear combination of CLS which changed their class from $U = 1$ to $U = 2$ (see Fig. 2). We observe sharp changes from an almost frozen state into an oscillating pattern due to Landau-Zener transitions at the gaps of

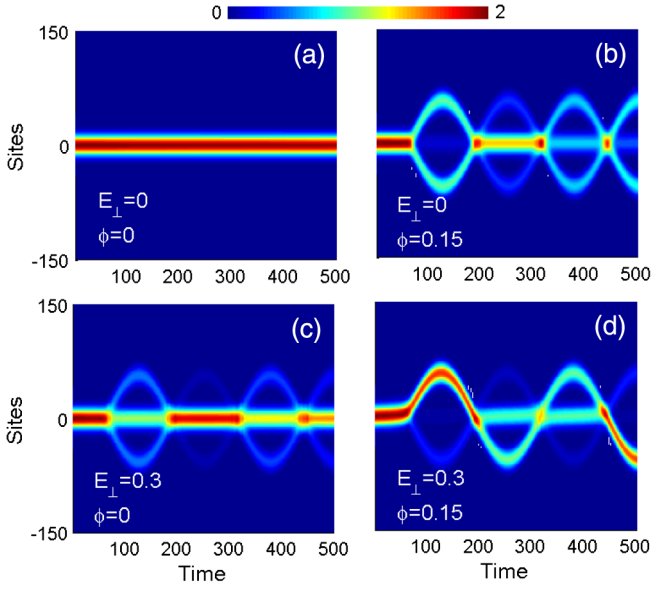

FIG. 4. Results of numerical simulations exciting initially a Gaussian CLS from in Fig. 2(a) (see text for details), with respective field values as taken in graphs of Fig. 3. In all simulations Graph (a) displays the case when transversal fields are absent, in (b) and (c) one of the fields is present, while in graph (d) both dc electric and magnetic fields are nonzero. $E_\parallel = 0.05$. The space-time evolution of the norm density $\rho_n = |a_n|^2 + |b_n|^2 + |c_n|^2$ is plotted in color code.

the band structure. These sudden switches from a nonmoving to a rapidly oscillating packet are further intensified and become asymmetric when both fields $E_\perp$ and ϕ turn nonzero, as seen in Fig. 4(d), respectively. Still the nonzero gap values induce a splitting of the wave packet—a part of the packet continues adiabatically, while a complementary part continues antiadiabatically due to Landau-Zener transitions.

Let us quantify these observations. Since we choose longitudinal field values $E_\parallel = 0.05$ which are small compared to the band structure width $2\sqrt{E_\perp^2 + 8}$ we can describe the Bloch oscillations by replacing k in the band structure for $E_\parallel = 0$ with the slow variable $E_\parallel t$ which scans the band structure. The starting point corresponds to the (almost) flat band in Figs. 3(b)–(d). The avoided crossings are reached at $k = \pi$ which translated into $t = \pi/E_\parallel = 63$ in excellent agreement with Figs. 4(b)–(d). The gap values are $\Delta = 0.18, 0.32, 0.16$ for the cases (b),(c),(d) in Fig. 3, respectively. The relevant Landau-Zener parameter α which describes the scanning speed through the avoided crossing is given by $\alpha = E_\parallel \sqrt{2}\cos^2(\phi/2)$ [35]. The probability $P = e^{-\pi\Delta^2/2\alpha}$ of a diabatic Landau-Zener transition [33] is then obtained as $P = 0.48, 0.1, 0.56$ for the cases (b),(c),(d) in Fig. 4. Indeed, the numerically observed diabatic transitions are much stronger in cases (b),(d) than the weaker one in case (c) in Fig. 4. This is a good approximation to the first observed passage of energy level crossings. Starting from the second passage one has to take into account the appearance of Stückelberg phases [36] which are responsible for constructive and destructive interference of wave functions. The analytical expressions for those phases as well as the respective tunneling probabilities for triple LZ tunneling are not available in closed form, but it is possible to evaluate these probabilities using Eq. (5) of the Supplemental Material [35].

We proceed to the case of vanishing gaps as discussed above. The most striking impact of both transversal dc electric and magnetic fields is that for $E_\perp = \sqrt{2}\sin\phi$, when the band structure turns gapless [Fig. 5(a)], Bloch oscillations harvest completely from Landau-Zener tunneling whose probability turns into unity. This case is displayed in Fig. 5(b) for an initial state given by a Gaussian envelope of the $k = 0$ lowest eigenenergy state from Fig. 5(a) with variance $\sigma = 70$ (such states can be, e.g., easily addressed with ultracold atomic condensates). For a significant part of its evolution it stands still, only to cross over into a large amplitude oscillation which clearly corresponds to the scanning of the corresponding band structure with complete Landau-Zener tunneling. These features are observed even in the case of an initial condition in the form a single CLS from Fig. 2(a) and shown in the lower plot in Fig. 5. In this case, the CLS remains essentially frozen until it performs a violent sweep through the system over about 30 sites, where it recombines only to perform the sweep again.

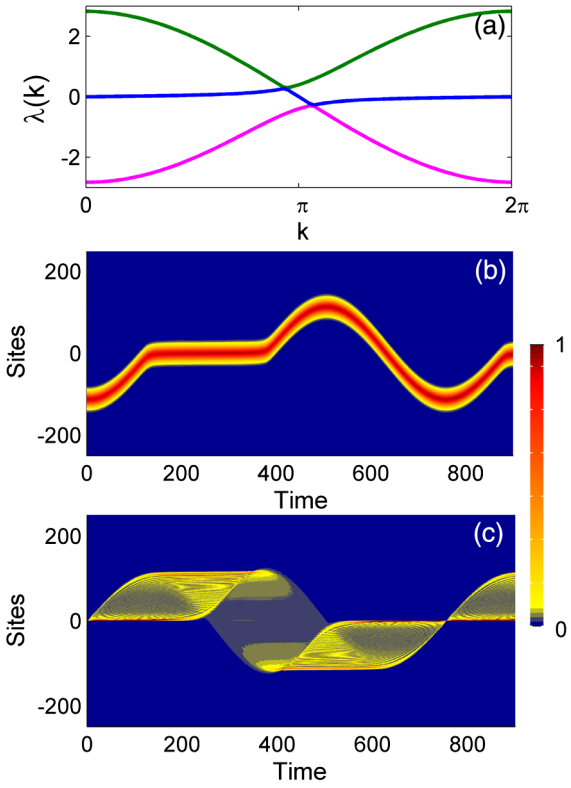

FIG. 5. The case $\phi = 0.2$ and $E_\perp = \sqrt{2}\sin\phi$. (a) Gapless band structure for $E_\parallel = 0$ demonstrating the complete gap closing. (b) The space-time evolution of the norm density $\rho_n = |a_n|^2 + |b_n|^2 + |c_n|^2$ for a Gaussian envelope of the $k = 0$ lowest eigenenergy state from the upper panel (a). Here $E_\parallel = 0.025$. (c) As in the middle panel (b), but the initial state is in the form of a pure single CLS shown in Fig. 2(a).

The combination of the physics of Bloch oscillations, Landau-Zener tunneling, and of flat band networks opens promising directions for control of unconventional quantum and photonic transport through properly designed lattice structures. Extensions of this study to two dimensions and to the inclusion of two-body interactions are intriguing pathways for further work.

R. Kh. acknowledges financial support from Georgian SRNSF (Grant No. FR/25/6-100/14) and travel grants from Georgian SRNSF and CNR, Italy (Grant No. 04/24) and CNRS, France (Grant No. 04/01).

[1] T. Brandes, Coherent and collective quantum optical effects in mesoscopic systems, Phys. Rep. **408**, 315 (2005).
[2] I. Bloch, J. Dalibard, and W. Zwerger, Many-body physics with ultracold gases, Rev. Mod. Phys. **80**, 885 (2008).
[3] M. Bellec, U. Kuhl, G. Montambaux, and F. Mortessagne, Tight-binding couplings in microwave artificial graphene, Phys. Rev. B **88**, 115437 (2013).

[4] D. N. Christodoulides, F. Lederer, and Y. Silberberg, Discretizing light behavior in linear and nonlinear waveguide lattices, Nature (London) **424**, 817 (2003).
[5] E. J. Bergholtz and Z. Lu, Topological flat band models and fractional Chern insulators, Int. J. Mod. Phys. B **27**, 1330017 (2013).
[6] A. Parameswaran, R. Roy, and S. L. Sondhi, Fractional quantum Hall physics in topological flat bands, C.R. Phys. **14**, 816 (2013).
[7] O. Derzhko and J. Richter, Universal low-temperature behavior of frustrated quantum antiferromagnets in the vicinity of the saturation field, Eur. Phys. J. B **52**, 23 (2006); O. Derzhko, J. Richter, A. Honecker, M. Maksymenko, and R. Moessner, Low-temperature properties of the Hubbard model on highly frustrated one-dimensional lattices, Phys. Rev. B **81**, 014421 (2010).
[8] M. Hyrkäs, V. Apaja, and M. Manninen, Many-particle dynamics of bosons and fermions in quasi-one-dimensional flat-band lattices, Phys. Rev. A **87**, 023614 (2013).
[9] O. Derzhko, J. Richter, and M. Maksymenko, Strongly correlated flat-band systems: The route from Heisenberg spins to Hubbard electrons, Int. J. Mod. Phys. B **29**, 1530007 (2015).
[10] D. Guzmán-Silva, C. Meijá-Cortés, M. A. Bandres, M. C. Rechtsman, S. Weimann, S. Nolte, M. Segev, A. Szameit, and R. A. Vicencio, Experimental observation of bulk and edge transport in photonic Lieb lattices, New J. Phys. **16**, 063061 (2014).
[11] R. A. Vicencio, C. Cantillano, L. Morales-Inostroza, B. Real, C. Meijia-Cortes, S. Weimann, A. Szameit, and M. I. Molina, Observation of Localized States in Lieb Photonic Lattices, Phys. Rev. Lett. **114**, 245503 (2015).
[12] S. Mukherjee, A. Spracklen, D. Choudhury, N. Goldman, P. Öhberg, E. Andersson, and R. R. Thomson, Observation of a Localized Flat-Band State in a Photonic Lieb Lattice, Phys. Rev. Lett. **114**, 245504 (2015).
[13] N. Masumoto, N. Y. Kim, T. Burnes, K. Kusudo, A. Löffler, S. Höfling, A. Forchel, and Y. Yamamoto, Exciton-polariton condensates with flat bands in a two-dimensional kagome lattice, New J. Phys. **14**, 065002 (2012).
[14] F. Baboux, L. Ge, T. Jacqmin, M. Biondi, A. Lemaitre, L. Le Gratiet, I. Sagnes, S. Schmidt, H. E. Türeci, A. Amo, and J. Bloch, Bosonic Condensation and Disorder-Induced Localization in a Flat Band, Phys. Rev. Lett. **116**, 066402 (2016).
[15] S. Taie, H. Ozawa, T. Ichinose, T. Nishio, S. Nakajima, and Y. Takahashi, Coherent driving and freezing of bosonic matter in an optical Lieb lattice, Sci. Adv. **1**, e1500854 (2015).
[16] G.-B. Jo, J. Guzman, C. K. Thomas, P. Hosur, A. Vishwanath, and D. M. Stamper-Kurn, Ultracold Atoms in a Tunable Optical Kagome Lattice, Phys. Rev. Lett. **108**, 045305 (2012).
[17] A. Mielke, Ferromagnetic ground states for the Hubbard model on line graphs, J. Phys. A **24**, L73 (1991); Ferromagnetism in the Hubbard model on line graphs and further considerations, J. Phys. A **24**, 3311 (1991); Exact ground states for the Hubbard model on the Kagome lattice, J. Phys. A **25**, 4335 (1992).
[18] H. Tasaki, Ferromagnetism in the Hubbard Models with Degenerate Single-Electron Ground States, Phys. Rev. Lett. **69**, 1608 (1992).
[19] R. G. Dias and J. D. Gouveia, Origami rules for the construction of localized eigenstates of the Hubbard model in decorated lattices, Sci. Rep. **5**, 16852 (2015).
[20] A. Nandy and A. Chakrabarti, Engineering flat electronic bands in quasiperiodic and fractal loop geometries, Phys. Lett. A **379**, 2876 (2015).
[21] D. L. Bergman, C. Wu, and L. Balents, Band touching from real-space topology in frustrated hopping models, Phys. Rev. B **78**, 125104 (2008).
[22] S. Flach, D. Leykam, J. D. Bodyfelt, P. Matthies, and A. S. Desyatnikov, Detangling flat bands into Fano lattices, Europhys. Lett. **105**, 30001 (2014).
[23] D. Leykam, J. D. Bodyfelt, A. S. Desyatnikov, and S. Flach, Localization of weakly disordered flat band states, arXiv: 1601.03784.
[24] J. D. Bodyfelt, D. Leykam, C. Danieli, X. Yu, and S. Flach, Flatbands under Correlated Perturbations, Phys. Rev. Lett. **113**, 236403 (2014).
[25] C. Danieli, J. D. Bodyfelt, and S. Flach, Flatband engineering of mobility edges, Phys. Rev. B **91**, 235134 (2015).
[26] H. L. Stormer, Nobel Lecture: The fractional quantum Hall effect, Rev. Mod. Phys. **71**, 875 (1999).
[27] J. Vidal, B. Doucot, R. Mosseri, and P. Butaud, Interaction Induced Delocalization for Two Particles in a Periodic Potential, Phys. Rev. Lett. **85**, 3906 (2000).
[28] B. P. Anderson and M. Kasevich, Macroscopic quantum interference from atomic tunnel arrays, Science **282**, 1686 (1998).
[29] M. Cristiani, O. Morsch, J. H. Müller, D. Ciampini, and E. Arimondo, Experimental properties of Bose-Einstein condensates in one-dimensional optical lattices: Bloch oscillations, Landau-Zener tunneling, and mean-field effects, Phys. Rev. A **65**, 063612 (2002).
[30] J. Struck, C. Ölschläger, M. Weinberg, P. Hauke, J. Simonet, A. Eckardt, M. Lewenstein, K. Sengstock, and P. Windpassinger, Tunable Gauge Potential for Neutral and Spinless Particles in Driven Optical Lattices, Phys. Rev. Lett. **108**, 225304 (2012).
[31] S. Longhi, M. Marangoni, M. Lobino, R. Ramponi, P. Laporta, E. Cianci, and V. Foglietti, Observation of Dynamic Localization in Periodically Curved Waveguide Arrays, Phys. Rev. Lett. **96**, 243901 (2006).
[32] M. Golshani, S. Weimann, Kh. Jafari, M. Khazaei Nezhad, A. Langari, A. R. Bahrampour, T. Eichelkraut, S. M. Mahdavi, and A. Szameit, Impact of Loss on the Wave Dynamics in Photonic Waveguide Lattices, Phys. Rev. Lett. **113**, 123903 (2014).
[33] L. D. Landau, Zur Theorie der Energieubertragung. II, Phys. Z. Sowjetunion **2**, 46 (1932); G. Zener, Non-adiabatic crossing of energy levels, Proc. R. Soc. A **137**, 696 (1932).
[34] G. H. Wannier, Wave functions and effective Hamiltonian for Bloch electrons in an electric field, Phys. Rev. **117**, 432 (1960).
[35] See Supplemental Material at http://link.aps.org/supplemental/10.1103/PhysRevLett.116.245301 for the calculation of extended mode interactions in the presence of longitudinal fields.
[36] S. N. Shevchenko, S. Ashhab, and F. Nori, Landau-Zener-Stückelberg interferometry, Phys. Rep. **492**, 1 (2010).